Effects of damping on surface-plasmon pulse propagation and refraction

Andreas Hohenau, Aurelien Drezet, Matthias Weißenbacher, Franz R. Aussenegg, and Joachim R. Krenn
Institute of Physics and Erwin Schrödinger Institute for Nanoscale Research, Karl-Franzens University, A-8010 Graz, Austria
(Received 21 August 2008; revised manuscript received 9 September 2008; published 6 October 2008)

We discuss the role of damping for surface-plasmon pulse propagation and refraction by analyzing calculated dispersion relations of a metal-dielectric interface. Results for a lossless Drude metal are compared to those for a lossy Drude metal and the application relevant materials gold and silver. We find that the imaginary part of the surface-plasmon wave vector rather than the surface-plasmon group velocity defines if normal or negative refraction takes place at lateral boundaries. As a consequence, the group velocity can be opposite to the energy flow. This is not in contradiction to causality, as due to large damping in regions of negative group velocities surface plasmons on a single interface are overdamped and evanescent in character. In addition, pulse spreading and the implications of the results for multilayer systems are discussed.

DOI: 10.1103/PhysRevB.78.155405 PACS number(s): 73.20.Mf, 42.25.Bs, 42.25.Fx, 73.21.−b

I. INTRODUCTION

Surface plasmons (SPs) are electromagnetic modes bound to the surface between a metal and a dielectric.[1,2] Among their special properties are their two-dimensional nature, subwavelength light confinement, and ultrafast decay. These lead to considering SPs as promising in nano-optical applications, for example, bridging the size mismatch between integrated optics and state-of-the-art integrated (opto)electronic devices.[3,4] Several SP optical functional devices such as waveguides, beam splitters, and multiplexers were demonstrated in the past. However, effects related to SP pulse propagation have not been discussed in detail, including group velocity and pulse spreading. In addition, SPs recently also proved highly interesting in connection to negative refraction.[5–9] Thin silver films were suggested[10] and experimentally demonstrated[11] to be capable of perfect lensing or superlensing across the film (see Ref. 12 for a recent review), with certain limitations.[13] Important and stimulating for this work were the reports of in-plane negative refraction of SPs at the lateral boundary between two different multilayer systems.[14–17] Such systems have one common metal layer which supports the SP, whose wavelength differs in the adjacent multilayer systems (i.e., the dispersion relations are different) and therefore SP refraction occurs. In the explanation of the observed negative refraction, only the real parts of the SP dispersion relations were considered as relevant for defining the direction of SP phase and group velocity and to identify frequency regions of negative refraction. However, this is only applicable if one considers SPs in a "transparency window,"[18,19] i.e., negligible propagation losses. With the strong damping SPs experience in realistic layer systems and published propagation length on the order of 50–100 nm,[16] this prerequisite is clearly not fulfilled. As detailed below, the SP refraction and pulse propagation can only be correctly described by considering both real and imaginary parts of the SP wave vector or dispersion relation, respectively.

The paper is structured as follows. First, we investigate SP pulses propagating along a single metal-dielectric interface in regions of positive and negative group velocities. To clarify the role of damping, we compare air interfaces of lossless and lossy Drude metals and application relevant metals silver and gold. Based on this, we then discuss the refraction (and possible negative refraction) of SP waves at a lateral boundary between two different metal-dielectric interfaces. Finally, the implications of our findings for SP propagation in multilayer systems are discussed.

II. SP PULSE PROPAGATION

In a laterally infinitely extended metal-layer system (or single metal-dielectric interface), the propagation of a somehow at one (infinitely distant) end excited SP is completely determined by its dispersion relation, i.e., the relation between the complex SP wave vector (describing the SP wavelength and propagation length) and the (real) frequency. For the SP pulse propagation, the sign and magnitude of phase and group velocity as well as propagation length, pulse spreading, and reshaping can be derived from the dispersion relation.[20] Similar to dielectric waveguides, this model is also applicable if the lateral extension of the layer system is finite but much larger than the SP wavelength.

A. Dispersion relation

In the following we consider a single metal-dielectric interface as that sketched in Fig. 1 and limit our discussion to nonmagnetic materials ($\mu=1$). The SP dispersion relation for such an interface is given by[1]

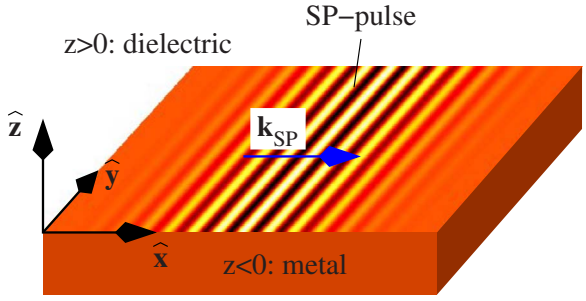

FIG. 1. (Color online) Sketch of the considered metal-dielectric interface. The SP pulse propagates along the $\hat{\mathbf{x}}$ direction.

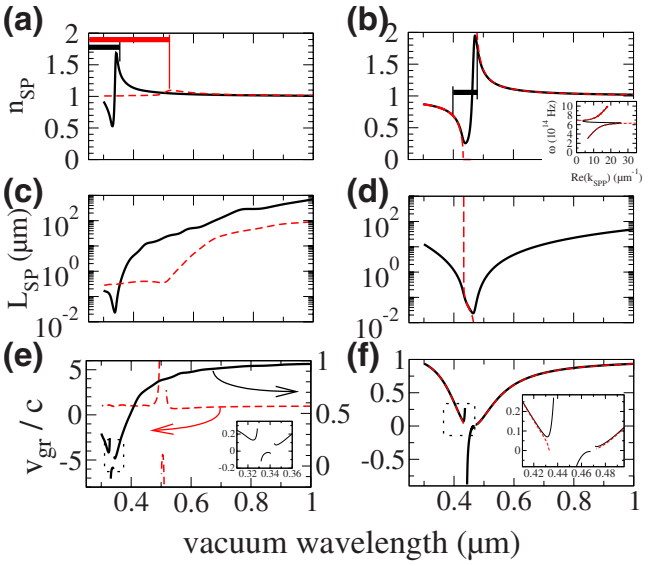

FIG. 2. (Color online) Dispersion relations of metal-air interfaces: SP effective indices n_{SP} [(a) and (b)], SP propagation lengths L_{SP} [(c) and (d)], and SP group velocities [(e) and (f)] of gold (red, dashed line) and silver (black, solid line) [(a) and (c)] and a Drude metal with $\Gamma=0$ (red, dashed line) and $\Gamma=0.08$ (black, solid line) [(b) and (d)]. The horizontal thick lines mark the regions where the SP propagation length L_{SP} is smaller than the SP wavelength. The inset in (b) shows the same dispersion relation as in (b) but in the "usual" representation of ω vs Re(k_{SP}). The group velocities [(e) and (f)] are plotted only in the range where Eq. (3) is valid for 100 fs SP pulses. Outside this range, SP pulse propagation cannot be described by a simple formulated group velocity. For the Drude metals the curves overlap in wide regions.

$$k_{SP}(\omega) = k'_{SP} + ik''_{SP} = k_0(\omega)\sqrt{\frac{\varepsilon_m(\omega)\varepsilon_d(\omega)}{\varepsilon_d(\omega)+\varepsilon_m(\omega)}}, \qquad (1)$$

where k_{SP} is the (complex) SP wave number, $k_0=\omega/c$ is the wave number of light in vacuum, and ε_d and $\varepsilon_m=\varepsilon'_m+i\varepsilon''_m$ are the permittivity functions of the dielectric and metal, respectively. The resulting dispersion relations for SPs at the interface of a lossless and lossy Drude metal, silver and gold, to air are plotted in Fig. 2. For the sake of clarity we chose to plot the effective SP index n_{SP} and propagation length L_{SP} [defined by $I_{SP}(x+L_{SP})=I_{SP}(x)e^{-1}$],

$$n_{SP} := k'_{SP}/k_0, \quad L_{SP} := 1/(2k''_{SP}), \qquad (2)$$

versus the vacuum wavelength $\lambda=2\pi/k_0$. As parameters for the Drude model ($\varepsilon_m=\varepsilon_\infty-\omega_p^2/[\omega(\omega+i\Gamma)]$), we used $\omega_p=7$ eV, $\Gamma=0.08$ eV or 0, and $\varepsilon_\infty=6$, which were chosen to give dispersion relations roughly similar to those of silver and gold.

In Fig. 2 the horizontal bars indicate regions where the calculated SP wavelength is larger than the SP propagation length and the SP behavior complies with more that of an evanescent wave than that of a propagating wave. For all investigated materials except the lossless Drude metal, the effective SP indices are below 2 and regions of anomalous dispersion are found but only in strongly damped, evanescent regimes. If the refractive index of the dielectric is increased (not shown), the maximum of n_{SP} increases and shifts toward larger wavelength. However the propagation length also decreases and the regions of anomalous dispersion are still strongly damped with propagation length below the SP wavelength.

B. Group velocity, phase velocity, and Poynting vectors

We now consider a one-dimensional SP wave packet, or pulse, respectively, moving along the $\hat{\mathbf{x}}$ direction on the interface (see Fig. 1). According to the Fourier theorem, this wave packet can be considered as a superposition of monochromatic homogeneous plane SP waves with their wave vectors parallel to $\hat{\mathbf{x}}$ ($\mathbf{k}_{SP}=k_{SP}\hat{\mathbf{x}}$). Due to the dispersion of the effective SP index, SP pulses will propagate along the interface with the group velocity[20,21]

$$v_{gr} = \frac{d\omega}{dk'_{SP}(\omega)} = \frac{c}{n_{SP}(\lambda) - \lambda\dfrac{dn_{SP}}{d\lambda}}, \qquad (3)$$

which can be calculated analytically from the dispersion relation. For the derivation of Eq. (3),[20] the dispersion relation expressed as $\omega(k_{SP})$ is developed into a Taylor series and all terms of order higher than 1 are dropped; i.e., their contributions have to be small compared to the linear term for the equation to hold. This condition not only depends on the dispersion relation but also on the pulse length (and therefore spectral width) of the considered SP pulses, which has to be small compared to the curvature of the dispersion curve. For example, for 100-fs-short SP pulses, the spectral width is sufficiently small for the above condition to be valid over most of the spectral range with the exception of the intervals with strong bending of n_{SP} before and after the regions of anomalous dispersion. Figures 2(e) and 2(f) depict the group velocities calculated by using Eq. (3) of SP pulses on a silver-air, a gold-air, and a Drude metal–air interface within its validity range. This was determined by checking if the contribution of the quadratic term to the series expansion of $\omega(k_{SP})$ is smaller than 1/10 of the linear term. Outside this region the strong bending of the dispersion relation leads to a more complicated pulse reshaping during propagation than just broadening and the concept of group velocity cannot be applied in a straightforward manner.[20] For shorter (longer) SP pulses, the validity range reduces (increases) further. It must be added that dispersion of the SP propagation length, or $k''_{SP}(\omega)$, also leads to distortions of the pulse in addition to damping, which is not considered in Eq. (3). Considerable differences in the propagation length within the spectral pulse width further limit the physical meaning of v_{gr} as defined by Eq. (3).

In all cases except for the lossless Drude metal, *negative* group velocities are observed, which appear in the regions of anomalous dispersion. The comparison with the lossless Drude metal shows that the existence of a region of negative group velocity is an effect of damping; i.e., negative group velocities are absent for SPs at lossless Drude metal–air interface. In the lossless case, this region is "forbidden" for the SP; i.e., the SP wave vector is purely imaginary, the effective index is zero, and the "propagation length" describes the

exponentially decreasing field of the evanescent, nonretarded SP wave. As soon as damping is added to the Drude model, the SP waves in the forbidden region get a propagative component to deliver the energy absorbed. However, the SPs keep their evanescent nature with a propagation length still smaller than their wavelength. For the experimental values of the silver or gold dielectric function, the behavior is similar to the damped Drude metal.

C. Energy flow and causality

In Sec. II B we could identify conditions where negative SP group velocity appears, i.e., where group velocity and phase velocity are antiparallel. We now want to clarify how the direction of group velocity is associated with the direction of energy flow and the Poynting vector.

For the following discussion it is convenient to consider both the real and imaginary parts of the SP wave vector [Eq. (1)] to derive

$$k'_{\mathrm{SP}}k''_{\mathrm{SP}} = \frac{1}{2}\frac{k_0^2\varepsilon''_m\varepsilon_d^2}{|\varepsilon_d+\varepsilon_m|^2} > 0. \tag{4}$$

This implies that as long as there is absorption in the metal ($\varepsilon''_m > 0$), the real and imaginary parts of the k_{SP} are always of the same sign. In other words, the phase velocity points toward the direction of exponential decay of the SP amplitude.

For the Poynting vectors, one can derive the following relations. Starting from the definition of the time averaged Poynting vector (in the Lorentz-Heaviside system of units) $\langle\mathbf{S}\rangle = c\frac{1}{2}\mathrm{Re}([\mathbf{E}\times\mathbf{H}^*])$ in combination with the TM polarized field of the SP propagating along $\hat{\mathbf{x}}$, i.e., $\mathbf{H}=(0,H_y,0)$ and $\mathbf{E}=(E_x,0,E_z)$, one finds

$$\langle S_x^j\rangle = c\frac{1}{2k_0}\mathrm{Re}\left(\frac{k_{\mathrm{SP}}}{\varepsilon_j}\right)e^{-2k''_{\mathrm{SP}}x-2k''_{z,j}z}$$

and

$$\langle S_z^j\rangle = c\frac{1}{2k_0}\mathrm{Re}\left(\frac{k_{z,j}}{\varepsilon_j}\right)e^{-2k''_{\mathrm{SP}}x-2k''_{z,j}z}, \tag{5}$$

with $j=$"m" (metal) or "d" (dielectric). Considering the fact that the SP wave is bound to the interface[22] the integration of $\langle S_x^j\rangle$ over the z direction in the metal and in the dielectric gives a finite value which represents the total-energy flux along the x direction in the two media.[23] The results are plotted in Fig. 3 and show that the x component of the energy flux is always positive (i.e., parallel to the k'_{SP}) in the dielectric (dash-dotted lines) but negative in the metal (dashed lines) over most of the spectral range (excluding the region in the vicinity of the absorption band) and for all materials considered. Integrating over the entire z direction leads to an overall positive x component of the energy flux $\langle S_x^{\mathrm{total}}\rangle = \int_{-\infty}^{0}\langle S_x^m\rangle dz + \int_0^{+\infty}\langle S_x^d\rangle dz$ (solid line), *also* in regions of negative group velocity (see Appendix A for the proof):

$$\langle S_x^{\mathrm{total}}\rangle = \frac{ce^{-2k''_{\mathrm{SP}}x}}{2k_0}\left[\frac{k'_{\mathrm{SP}}}{2k''_{z,d}\varepsilon_d} - \frac{k'_{\mathrm{SP}}\varepsilon'_m + k''_{\mathrm{SP}}\varepsilon''_m}{2k''_{z,m}|\varepsilon_m|^2}\right] > 0. \tag{6}$$

This in turn shows that although there is a part of the dispersion relation with negative group velocity, the total-energy flow is always in the same direction as the phase velocity and the direction of exponential SP decay. The latter is also qualitatively intuitive: if the energy flow would be opposite to the direction of exponential decay of the SP wave, the SP would gain intensity with increasing propagation distance. In the current case where only absorbing media without gain are involved, this would violate causality (this point is justified in Appendix A). Further, the parallelism between the Poynting vector and phase velocity implies that in the frequency range of negative group velocity, the Poynting vector and energy flow are *opposite* to the group velocity. In other words, the phase velocity is always positive with respect to the direction of energy flow.

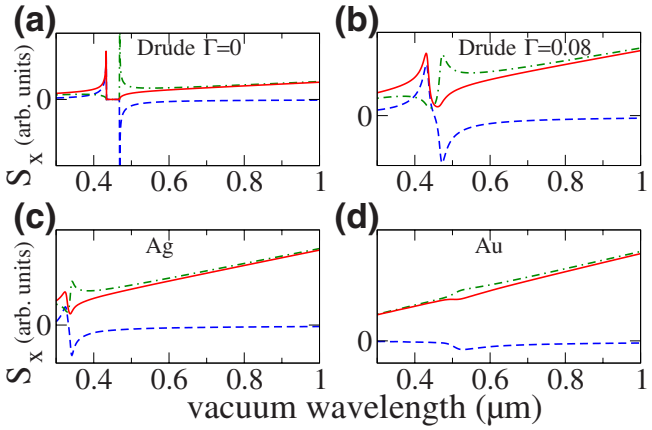

FIG. 3. (Color online) Components of the time averaged Poynting vectors parallel to the metal-dielectric interface and integrated in the z direction over the metal region (blue, dashed lines), the dielectric region (green, dash-dotted lines), and the sum of both (red, solid lines) for SP at the air interface of a lossless Drude metal (a), a Drude metal with damping (b), silver (c), and gold (d).

This behavior in regions of anomalous dispersion may seem counterintuitive at first sight. This is caused by describing the SP behavior in an evanescent regime with the language of propagating waves. To illustrate the situation, we plot in Fig. 4 the intensity of a SP pulse on a silver-air interface over propagation distance x and time at 336 nm [negative group velocity, Figs. 4(a), 4(c), and 4(e)] and 600 nm [positive group velocity, Figs. 4(b), 4(d), and 4(f)]. As can be seen from Fig. 4(c), the negative group velocity does not violate causality in this strongly damped case, as the intensity at larger x is never larger than at smaller x at a given time, although the intensity maximum appears earlier at larger x [Fig. 4(e)].

As the last point in the discussion of SP pulse propagation on a single interface, we consider the SP pulse spreading during propagation. In Fig. 4 no obvious pulse spreading can be observed within the propagation distance of the pulse. A rough estimate of the pulse broadening can be derived by considering the pulse as a superposition of several spectrally more narrow pulses, which propagate at different group velocities.[20] The spatial pulse width $l(t)$ as a function of pulse travel time t can then be approximated as[20]

$$l(t) \simeq \sqrt{l_0^2 + (d^2\omega/dk_{\mathrm{SP}}^2\Delta k_{\mathrm{SP}}t)}. \tag{7}$$

The results of this estimation show that (in the regions where the group-velocity concept can be applied) even for SP

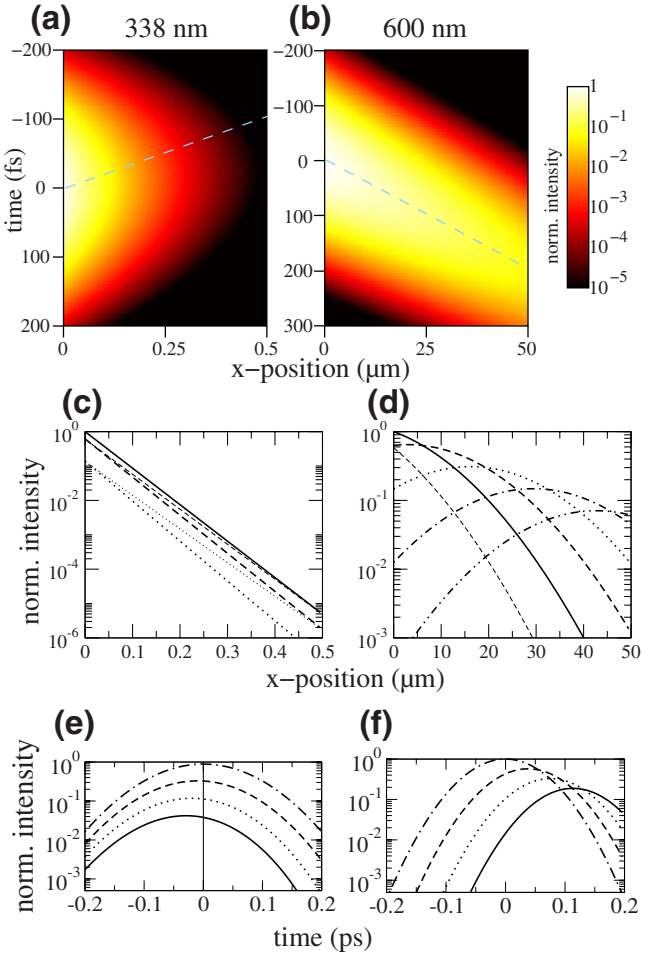

FIG. 4. (Color online) Plots of the SP intensity over time and propagation distance x for a 100 fs Gaussian SP pulse at a silver-air interface at center vacuum wavelengths of 338 (a) and 600 nm (b). The blue, dashed lines indicate the group velocities as calculated by Eq. (3). (c) and (d) represent horizontal cuts through (a) and (b), respectively, i.e., SP intensity vs propagation distance diagrams for different times (−50 fs: thin dotted line; −25 fs: thin dashed line; 0 fs: thick solid line; 25 fs: thick dashed line; 50 fs thick dotted line; 100 fs: thin dash-dotted line; 150 fs: thick dashed-double-dotted line). Whereas at 600 nm the pulse maximum moves toward larger x with increasing time, the pulse at 338 nm is always exponentially decaying toward larger x. However, the exponential decay is stronger at later times than at earlier times, whereby the pulse deforms in a way that its maximum appears earlier at larger x. This behavior is more clearly visible in (e), which represents vertical cuts through (a) at different positions: 0 nm (dash-dotted line), 50 nm (dashed line), 100 nm (dotted line), and 150 nm (solid line). (f) shows vertical cuts through (b): 0 (dash-dotted line), 10 μm (dashed line), 20 μm (dotted line), and 30 μm (solid line).

pulses as short as 10 fs, the pulse spreading is negligible small over the SP $1/e$ propagation length.[24] Therefore, in Fig. 4 no pulse spreading can be observed.

It is interesting to remark that the limitations mentioned above in the context of SPs, concerning the meaning of v_{gr} close to or in an "absorption" band, are already known in the context of wave propagation in bulk.[20,21,25–31] In a region of anomalous dispersion where $|\varepsilon'| \sim |\varepsilon''|$, it is generally not possible to identify v_{gr} with v_E, defined as the rate of energy flow divided by the stored energy density, and only when $|\varepsilon''| \ll |\varepsilon'|$ is this identification justified.[18,20,32] The fact that $v_{\mathrm{gr}} < 0$ (and $|v_{\mathrm{gr}}| > c$) does not then lead to any paradoxes shows how cautious one should be in using the concept of group velocity to predict the existence of a negative refraction regime (a point which was already emphasized by Lamb[5] in 1904).

III. SP REFRACTION

In view of recent publications reporting on negative refraction of SPs in regions of negative group velocities,[14,16,17] it is interesting to further investigate the possible SP refraction for the current case. For our simple model of semi-infinite metal and dielectric perpendicular to the interface, SP refraction could occur if there is a lateral boundary of two regions located, say, at the plane $x=0$, separating different dielectrics and/or metals. This implies four media: two metals (with permittivities $\varepsilon_{m,1}$ and $\varepsilon_{m,2}$ located in the three-dimensional (3D) regions $[x<0, z<0]$ and $[x>0, z<0]$, respectively) and two dielectrics (with permittivities $\varepsilon_{d,1}$ and $\varepsilon_{d,2}$ located in the 3D regions $[x<0, z>0]$ and $[x>0, z>0]$, respectively). In such a system and at a given frequency, the $k_{\mathrm{SP}}(\omega)$ have different values [Figs. 5(a) and 5(b)] for both metal-dielectric interfaces. The modeling of SP refraction for that case is, as explained below, already complicated and a detailed, quantitative description can only be achieved by numerical methods. However, the continuity relations for the field also have to hold along a lateral boundary. Therefore, by knowing the dispersion relations on both sides of the boundary, one can in principle determine the angles and character (normal or negative) of SP refraction.

Let us recall the conditions required to observe negative SP refraction: negative refraction occurs if the direction of energy flow is opposite to the SP phase velocity at one side (e.g., the refraction side) of the boundary for the given frequency. This is because continuity requires the component k_y of $\mathbf{k}_{\mathrm{SP}}$ parallel to the boundary to be conserved across it, but causality requires that the energy propagate toward the boundary from the excitation side and away from the boundary on the other (refraction) side. Since the energy flow is opposite to the phase velocity, at the refraction side the direction of the component k_x of $\mathbf{k}_{\mathrm{SP}}$ perpendicular to the boundary is determined to point toward the interface.

This intuitive picture of negative refraction (which is applicable for lossless media) is however already an oversimplification of the problem. First, SP waves do not constitute a complete and orthogonal vectorial mode basis to describe electromagnetic wave propagation at an interface. This means that additional TE and TM modes would have to be taken into account in a full description including not only SP reflection and refraction but also the out-of-plane scattering (i.e., typically ~20% of the total energy).[33,34] Second, the continuity conditions imposed on the wave-vector component k_y at the lateral boundary are rigorously satisfied only if k_y is a real number, i.e., if we use a Fourier series expansion. Usual homogeneous SP plane waves characterized by a complex in-plane wave vector $k_{\mathrm{SP}}\hat{\mathbf{n}} = k_{\mathrm{SP}}[\cos(\theta)\hat{\mathbf{x}} + \sin(\theta)\hat{\mathbf{y}}]$, in

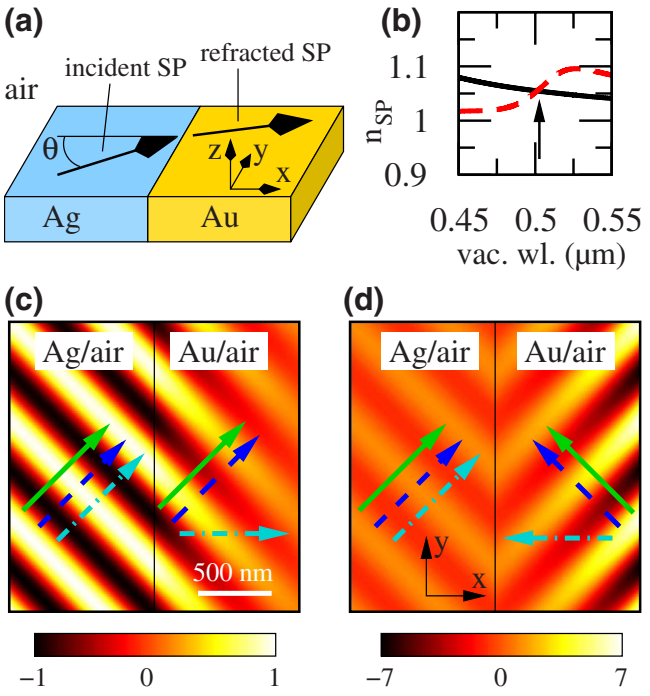

FIG. 5. (Color online) Sketch of a SP incident on a lateral boundary oriented along y between a silver-air and a gold-air interface (a). Details of the SP dispersion relations of the Ag-air (black, solid line) and Au-air (red, dashed line) interface (b). The arrow indicates the wavelength of 501 nm, at which $n_{\mathrm{SP,Ag}}=1.0539 \simeq n_{\mathrm{SP,Au}}=1.0549$ but $v_{\mathrm{gr,Ag}}/c=0.81$ and $v_{\mathrm{gr,Au}}/c=-6.6$. The propagation lengths are $L_{\mathrm{SP,Ag}}=21$ μm and $L_{\mathrm{SP,Au}}=355$ nm. Φ_{SP} field strength of the incident (normalized to 1) and refracted SPs (c). The reflected SP and light scattering are not considered. Solid, green arrows: k'_{SP}; dashed, blue arrows: energy flow; dash-dotted, turquoise arrows: k''_{SP}. (d) is same as (c) but for the hypothetical case, where negative refraction would occur. We remark that the SP propagation length along the x direction on the gold side [i.e., $L_x=1/(2k''_x)$] has a value of 255 nm, which is even smaller than the value L_{SP} deduced from Eq. (2).

which k_{SP} is given by Eq. (1) and θ is a real number, do not in general satisfy this condition (specifically not in a region of anomalous dispersion, where damping is strong). However, there are formal mathematical solutions to this problem if we expand the TE and TM waves into a set of different adapted modes. The method is briefly summarized in Appendix B. Here what is essential is that SP waves are completely characterized by the knowledge of the scalar function $\Phi_{\mathrm{SP}}(x,y)$ which can be expanded as

$$\Phi_{\mathrm{SP}}(x,y)=\sum_{\pm}\int_{-\infty}^{+\infty}dk_y a_{\pm}(k_y)e^{i(k_y y+k_{x,\pm}x)}, \tag{8}$$

where k_y is a real number and $k_{x,\pm}=\pm\sqrt{(k_{\mathrm{SP}}^2-k_y^2)}$ is complex valued. The phase matching condition over k_y at the lateral boundary $x=0$ allows us to define the refraction and reflection laws for SPs. We apply this model for the following analysis and we emphasize that no reflection, transmission, or scattering coefficients are here determined from this.

Exemplarily we consider a lateral boundary oriented along y of a silver and gold surface [Fig. 5(a)]. The common superstratum is here chosen to have $\varepsilon_{d,1}=\varepsilon_{d,2}=1$ (i.e., air or vacuum). The incoming SP with a wave vector $k_{\mathrm{SP}}[\cos(\theta)\hat{\mathbf{x}}+\sin(\theta)\hat{\mathbf{y}}]$ hits the boundary from the silver side at inclined incidence. The vacuum wavelength is chosen to be 501 nm, where $n_{\mathrm{SP,Ag}}\simeq n_{\mathrm{SP,Au}}$ but $v_{\mathrm{gr,Ag}}>0$ and $v_{\mathrm{gr,Au}}<0$, so that negative SP refraction could be expected if only the real parts of the SP wave vectors or SP indices, respectively, are considered. For normal incidence ($\theta=0$), according to the results in Sec. II, it is already clear that negative SP refraction cannot occur: $k_y=0$, the SP waves are homogeneous, and the energy flow is always parallel to the SP phase velocity. The SP refractive index therefore has to be considered as positive over the entire spectral range, independent of the group velocity.

For inclined SP incidence ($\theta\neq 0$), it can be shown that the conclusion is actually the same. To understand this nontrivial result, we first point out that due to the presence of losses the transmitted plane wave on the gold side is generally not homogeneous. In other words the problem leads to a wave where lines of constant phase are not lines of constant intensity anymore; i.e., $\mathbf{k}'_{\mathrm{SP}}$ is parallel neither to $\mathbf{k}''_{\mathrm{SP}}$ nor to the in-plane energy flow.[35] This is clearly visible in Figs. 5(c) and 5(d), where we plot for $\theta=45°$ (Ref. 36) how the SP Φ_{SP} field of the incident and refracted waves (reflected SP and scattered light are not considered) would look for normal, positive (c), and negative (d) refractions. Clearly the refracted SP waves are laterally decaying along the $\pm x$ direction. Importantly, due to the (near[35]) parallelism between the Poynting vector and phase velocity and because the angle between $\mathbf{k}'_{\mathrm{SP}}$ and $\mathbf{k}''_{\mathrm{SP}}$ is smaller than 90° in the refraction side, negative refraction would require an exponentially growing SP intensity with increasing distance from the boundary and energy flowing from the refraction side toward the boundary [Fig. 5(d)], which clearly violates causality.

The conclusions obtained from this particular example are actually very general. Indeed, for an inhomogeneous SP plane wave with wave vector $\mathbf{k}_{\mathrm{SP}}=\mathbf{k}'_{\mathrm{SP}}+i\mathbf{k}''_{\mathrm{SP}}$ along the interface, it is possible to show (Appendix C) that as long as $\varepsilon''_m>0$, we have

$$\mathbf{k}'_{\mathrm{SP}}\cdot\mathbf{k}''_{\mathrm{SP}}>0, \quad \mathbf{k}''_{\mathrm{SP}}\cdot\langle\mathbf{S}^{\mathrm{total}}\rangle\gg 0. \tag{9}$$

Since in the TM basis considered [see Eq. (8)] $\mathbf{k}''_{\mathrm{SP}}=k_x\hat{\mathbf{x}}=\pm\sqrt{(k_{\mathrm{SP}}^2-k_y^2)}\hat{\mathbf{x}}$, this implies that for each individual transmitted SP we have $k'_x k''_x>0$ and $k''_x\langle S_x^{\mathrm{total}}\rangle<0$. Now, with the same geometrical convention than before negative refraction can only hold if in the refraction side $k_x<0$. This consequently would also require $\langle S_x^{\mathrm{total}}\rangle<0$ and $k''_x<0$, that is, an energy flow moving in the direction of the lateral interface together with a field amplitude growing away from it. This completely noncausal behavior demonstrates that negative refraction is actually forbidden in the considered system.

IV. CONCLUSION

From the above analysis one can extract that for SPs on a single interface: (1) anomalous dispersion and negative group velocities arise from Ohmic damping in the metal and

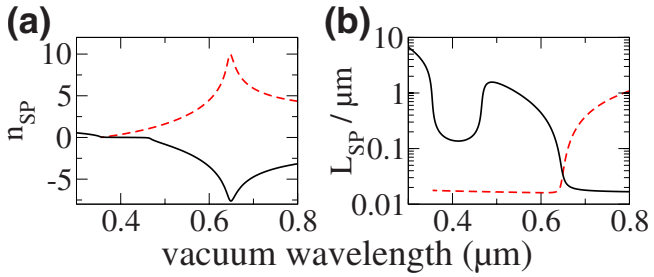

FIG. 6. (Color online) Dispersion relations of the asymmetric (black, solid line) and symmetric (red, dashed line) SP modes of a 50-nm-thick dielectric layer between two semi-infinite, lossy Drude metals. Effective refractive index (a) and propagation length (b). The effective index is plotted as negative if the energy flow is opposite to the phase velocity or, equivalently, if the real and imaginary parts of k_{SP} have opposite signs. The symmetry refers to the magnetic fields.

are absent for lossless Drude metals; (2) negative group velocities are not necessarily connected to negative refraction and an energy flow, or the Poynting vector, opposite to the phase velocity; (3) the SPs are evanescent in nature at the anomalous dispersion region; and (4) pulse spreading due to bending of the dispersion relation is not relevant over the SP propagation length. The question arises as to how these properties of SP pulses are modified by considering more than one interface. Generally, the findings from above cannot be extended to arbitrary layer systems as, for example, modes with anomalous dispersion exist also for lossless Drude metals for a single metal film between two extended dielectrics[37] or a dielectric film between two extended metals.[38] The nature of such modes, i.e., if they are evanescent, overdamped, or propagating modes, as well as the relevance of pulse spreading, can only be answered for the specific layer system under consideration. The results presented here can be applied as good approximation for SPs on not too thin metal films (thickness larger than ~70 nm for silver or gold) and SPs on such metal films loaded with dielectric layers with thicknesses larger than the $1/e$ extension of the evanescent fields. However, the fact that the group velocity is, due to losses, not linked to the direction of energy flow and unsuitable for the identification of negative refraction regions, can be extended to any (SP) mode in any layer system.

As an example, we plot in Fig. 6 the dispersion relation of the asymmetric (black, solid line) and symmetric (red, dashed line) SP modes of a 50-nm-thick dielectric layer between two semi-infinite, lossy Drude metals.[14,37] To obtain the dispersion relation, we numerically solved the dispersion relation to a precision of 10^{-10} (Ref. 39) and used $\omega_p = 3.5$ eV, $\Gamma = 0.04$ eV, and $\varepsilon_\infty = 1$ as parameters for the Drude model. The effective refractive index is plotted negative if the real and imaginary parts of k_{SP} have opposite signs. This is equivalent to opposite signs of energy flow and phase velocity, which was confirmed by numerically integrating the parallel component of the Poynting vectors along a line perpendicular to the interfaces. Both modes have regions of positive and negative group velocities (normal and anomalous dispersions). The symmetric mode has a positive effective index over the entire considered spectral range and is of evanescent nature in the region of negative group velocity, similar to the SP mode on a single interface. In contrast, the asymmetric mode has negative effective index over most of the considered spectral range, and is propagative only in the region of negative group velocity (or anomalous dispersion).

This highlights that if there is absorption in the layer system, causality requires that the electromagnetic fields decay with propagation, i.e., with increasing distance from the source and in the direction of energy flow. Negative refraction is related to opposite signs of energy flow and phase velocity and therefore to an opposite sign of the real and imaginary parts of the complex SP wave vector, whereas the group velocity is only relevant for identification of negative refraction in the absence of absorption.

APPENDIX A

The conditions for the existence of negative refraction in a dissipative bulk medium have been recently obtained.[40–45] It can indeed be shown that the dispersion relation $k^2 = (k' + ik'')^2 = k_0^2 \varepsilon \mu$ for a plane wave with wave vector $\mathbf{k} = k\hat{\mathbf{x}}$ propagating in a medium with permittivity $\varepsilon = \varepsilon' + i\varepsilon''$ and permeability $\mu = \mu' + i\mu''$ implies the equation

$$k'k'' = \frac{1}{2}k_0^2(\varepsilon'\mu'' + \varepsilon''\mu'). \tag{A1}$$

Additionally the time averaged Poynting vector for such a wave is $\langle S \rangle = \frac{c}{2k_0}\mathrm{Re}[\frac{k}{\mu}]|\mathbf{E}|^2$ from which we deduce

$$k'\langle S \rangle \propto \varepsilon'|\mu| + |\varepsilon|\mu',$$

$$k''\langle S \rangle \propto \varepsilon''|\mu| + |\varepsilon|\mu'' \tag{A2}$$

(the multiplicative constant omitted in this appendix are always positive). Negative refraction occurs if $k'\langle S \rangle < 0$.[40] Similarly $k''\langle S \rangle$ measures the passivity of the system (i.e., the medium is passive if $\varepsilon''|\mu| + |\varepsilon|\mu'' > 0$ and active if $\varepsilon''|\mu| + |\varepsilon|\mu'' < 0$). Comparisons between Eq. (A1) and Eq. (A2) show that the signs of k', k'', and $\langle S \rangle$ are interdependent:

$$\mathrm{sgn}[k'\langle S \rangle] = \mathrm{sgn}[k''\langle S \rangle]\mathrm{sgn}[k'k''], \tag{A3}$$

since $k'\langle S \rangle = k''\langle S \rangle \frac{k'^2}{k''k'}$. In particular in a doubly passive medium (i.e., $\varepsilon'' < 0$ and $\mu'' < 0$) $\mathrm{sgn}[k'\langle S \rangle] = \mathrm{sgn}[k'k'']$ (Refs. 40 and 45) so that negative refraction is possible if $k'k'' < 0$ (e.g., $\mu' < 0$ and $\varepsilon' < 0$). Physically it means that negative refraction in a passive medium implies that the wave is exponentially growing in the direction of the phase velocity $\mathbf{v}_p = \omega/|k'|\mathbf{k}'/|k'|$ and in the direction opposite to $\langle \mathbf{S} \rangle$. We show in the following that relations similar to Eqs. (A1)–(A3) exist for SPs. Here we consider only the case $\mu = 1$ and $\varepsilon'' > 0$ (calculations for the lossless case $\mu'' = \varepsilon'' = 0$ were recently done[7]). We consider in this appendix the case of a homogeneous SP plane wave with $\mathbf{k}_{SP} = k_{SP}\hat{\mathbf{x}}$. First, Eq. (4) plays the role of Eq. (A1) and we have $k'_{SP}k''_{SP} > 0$. Second, the time averaged Poynting vector along the interface is $\langle S_x^j \rangle \propto \mathrm{Re}[k_{SP}/\varepsilon_j]$, with $j = m$ or d. To simplify the notation we use the "tilde" variables $\tilde{\varepsilon} = \varepsilon_m/\varepsilon_d$, $\tilde{k}_{SP} = k_{SP}/\varepsilon_d$, $\tilde{k}_{z,j} = k_{z,j}/\varepsilon_d$,

and $\langle \tilde{S}_x^j \rangle \propto \mathrm{Re}[\tilde{k}_{\mathrm{SP}}/\tilde{\varepsilon}_j] e^{-2k''_{\mathrm{SP}}x - 2k''_{z,j}z}$ (i.e., $\langle \tilde{S}_x^m \rangle \propto (\tilde{k}'_{\mathrm{SP}}\tilde{\varepsilon}' + \tilde{k}''_{\mathrm{SP}}\tilde{\varepsilon}'') e^{-2k''_{\mathrm{SP}}x - 2k''_{z,j}z}/|\tilde{\varepsilon}|^2$ and $\langle \tilde{S}_x^d \rangle \propto \tilde{k}'_{\mathrm{SP}} e^{-2k''_{\mathrm{SP}}x - 2k''_{z,j}z}$). With this set of parameters we deduce[22]

$$\langle \tilde{S}_x^{\mathrm{total}} \rangle = \int_{-\infty}^{0} \langle \tilde{S}_x^m \rangle dz + \int_{0}^{+\infty} \langle \tilde{S}_x^d \rangle dz \propto \frac{1}{2}\left(- \frac{\tilde{k}'_{\mathrm{SP}}\tilde{\varepsilon}' + \tilde{k}''_{\mathrm{SP}}\tilde{\varepsilon}''}{|\tilde{\varepsilon}|^2 \tilde{k}''_{z,m}} + \frac{\tilde{k}'_{\mathrm{SP}}}{\tilde{k}''_{z,d}} \right) e^{-2k''_{\mathrm{SP}}x}. \tag{A4}$$

Multiplication of this expression by $\tilde{k}''_{z,d}\tilde{k}''_{\mathrm{SP}}$ and use of the equalities $\tilde{k}''_{z,d}\tilde{k}'_{z,d} = -\tilde{k}''_{\mathrm{SP}}\tilde{k}'_{\mathrm{SP}}$, $\tilde{k}_{z,d} = \tilde{k}_{z,m}/\tilde{\varepsilon}$ with the conditions $\tilde{k}''_{z,d} > 0$ and $\tilde{k}''_{z,m} > 0$ (Ref. 22) lead to the relation

$$\tilde{k}''_{\mathrm{SP}} \langle \tilde{S}_x^{\mathrm{total}} \rangle \propto (\tilde{k}''_{z,d}\tilde{k}''_{\mathrm{SP}})^2 + (\tilde{k}''_{\mathrm{SP}}\tilde{k}'_{\mathrm{SP}})^2 \tilde{\varepsilon}'' > 0 \tag{A5}$$

since $\tilde{\varepsilon}'' > 0$. From Eqs. (4) and (A5) we finally deduce

$$\tilde{k}'_{\mathrm{SP}} \langle \tilde{S}_x^{\mathrm{total}} \rangle = \tilde{k}''_{\mathrm{SP}} \langle \tilde{S}_x^{\mathrm{total}} \rangle \frac{\tilde{k}'^2_{\mathrm{SP}}}{\tilde{k}''_{\mathrm{SP}}\tilde{k}'_{\mathrm{SP}}} > 0, \tag{A6}$$

which shows that the SP wave decays in the same direction than $\tilde{k}'_{\mathrm{SP}}$ and $\langle \tilde{S}_x^{\mathrm{total}} \rangle$ or in other words the impossibility of negative refraction in the considered system. It can be added that a direct evaluation of $\tilde{k}'_{\mathrm{SP}} \langle \tilde{S}_x^{\mathrm{total}} \rangle$ gives

$$\tilde{k}'_{\mathrm{SP}} \cdot \langle \tilde{S}_x^{\mathrm{total}} \rangle \propto \tilde{k}'^2_{\mathrm{SP}} \tilde{k}''^2_{z,d} \tilde{\varepsilon}' (1 - |\tilde{\varepsilon}|^2) + \tilde{k}'_{\mathrm{SP}}\tilde{k}''_{\mathrm{SP}}\tilde{\varepsilon}''(\tilde{k}''^2_{z,d} + |\tilde{\varepsilon}|^2 \tilde{k}'^2_{\mathrm{SP}}). \tag{A7}$$

This function is obviously always positive if $\tilde{\varepsilon}' < 0$ and $|\varepsilon| > 1$ and a numerical calculation on the complex plane $(\tilde{\varepsilon}', \tilde{\varepsilon}'')$ shows that it is actually also true whatever $\tilde{\varepsilon}$ (including media with gain) is.

APPENDIX B

We remind that a general TE and TM mode expansion can be obtained with respect to the z axis. In each medium considered the field at the location $\mathbf{r} = [x, y, z]$ can indeed be written,[28,46]

$$\mathbf{E}(\mathbf{r}) = \nabla \times [\psi_{\mathrm{TE}}(\mathbf{r})\hat{\mathbf{z}}] - \nabla \times \nabla[\psi_{\mathrm{TM}}(\mathbf{r})\hat{\mathbf{z}}]/(ik_0\varepsilon),$$

$$\mathbf{H}(\mathbf{r}) = \nabla \times [\psi_{\mathrm{TM}}(\mathbf{r})\hat{\mathbf{z}}] + \nabla \times \nabla[\psi_{\mathrm{TE}}(\mathbf{r})\hat{\mathbf{z}}]/(ik_0), \tag{B1}$$

where the two scalar functions $\psi_{\mathrm{TM}}(\mathbf{r})$ and $\psi_{\mathrm{TE}}(\mathbf{r})$ obey the Helmholtz equation $[\nabla^2 + k_0^2\varepsilon]\psi(\mathbf{r}) = 0$. An adapted modal representation for the fields is obtained by expanding them as Rayleigh integrals:

$$\psi(\mathbf{r}) = \sum_{\pm} \int f_{\pm}(k_x, k_y) e^{i(k_x x + k_y y + k_{z,\pm} z)} dk_x dk_y, \tag{B2}$$

where k_x and k_y are real numbers and where $k_{z,\pm} = \pm\sqrt{(k_0^2\varepsilon - k_x^2 - k_y^2)}$ is complex valued. Equations (B1) and (B2) together with the boundary conditions at the interfaces can in general be used to solve numerically the problem and define the reflection, transmission, or scattering coefficients.[28,34] The expansion given by Eq. (B2) has two advantages. The first is that since k_y is a real number the conditions of phase matching at the boundary $x = 0$ are automatically satisfied along the y direction for the elementary modes (even though it is not the case in the z direction). This means that if we come with an incident wave characterized by a given k_y, the reflected and transmitted waves will be characterized by the same value of k_y. The second advantage is that this expansion contains SP waves as a particular case of the TM field. Indeed, by definition SP waves are TM modes bound to the surface and are characterized by the scalar function $\psi_{\mathrm{SP}}(\mathbf{r}) = f(z)\Phi_{\mathrm{SP}}(x, y)$, where $f(z)$ must decrease rapidly in both the $+z$ and $-z$ directions away from the metal/dielectric interface. Separation of the variables in the Helmholtz equation and boundary conditions lead to $f(z) = e^{ik_{z,m}z}$ in the metal and $f(z) = e^{ik_{z,d}z}$ in the dielectric and to the usual SP condition:[1] $k_{z,m}/\varepsilon_m = k_{z,d}/\varepsilon_d$. The function $\Phi_{\mathrm{SP}}(x, y)$ obeys the equation $[\partial^2/\partial x^2 + \partial^2/\partial y^2 + k_{\mathrm{SP}}^2]\Phi_{\mathrm{SP}}(x, y) = 0$, where k_{SP} is given by Eq. (1). An alternative representation to Eq. (B2) for ψ_{SP} is

$$\psi_{\mathrm{SP}}(\mathbf{r}) = e^{ik_{z,j}z} \sum_{\pm} \int_{-\infty}^{+\infty} d\tilde{k}_y a_{\pm}(\tilde{k}_y) e^{i(\tilde{k}_y y + \tilde{k}_{x,\pm} x)}, \tag{B3}$$

where $\tilde{k}_y$ is a real number and $\tilde{k}_{x,\pm} = \pm\sqrt{(k_{\mathrm{SP}}^2 - \tilde{k}_y^2)}$ is complex valued. The advantage of Eq. (B3) over Eq. (B2) is that it contains only one k_z so that the SP evanescent structure appears explicitly. Additionally, Eq. (B3) can be easily combined with expansion (B2) for the scattering contributions. In particular the phase matching condition at the boundary $x = 0$ keeps the same form for scattered light and for SPs since at a given $\tilde{k}_y$ an elementary SP mode $e^{i(\tilde{k}_y y + \tilde{k}_{x,\pm} x)}$ has a representation in Eq. (B2) leading to the amplitude coefficients $f(k_x, k_y) \sim \delta(\tilde{k}_y - k_y) g(\tilde{k}_x, k_x)$, where $\delta(u)$ is the Dirac function and where $g(\tilde{k}_x, k_x)$ is a narrow function centered on the value $k_x \simeq \mathrm{Re}[\tilde{k}_x]$. This means that if our aim is only to derive the refraction and reflection laws, i.e., the equivalent of Snell's laws, for SP waves, then we can completely ignore the out-of-plane scattering from our analysis.

APPENDIX C

For a general SP plane wave (homogeneous or not) with wave vector $\mathbf{q}_j = \mathbf{k}_\parallel + k_{z,j}\hat{\mathbf{z}}$ in the medium j, the magnetic field at $\mathbf{r} = [\mathbf{r}_\parallel, z]$ reads $\mathbf{H}_j(\mathbf{r}) = \hat{\mathbf{b}}_{\parallel,j} e^{i(\mathbf{q}_j \cdot \mathbf{r} - \omega t)}$, where $\hat{\mathbf{b}}_{\parallel,j} = \mathbf{q} \times \hat{\mathbf{z}}/|k_\parallel| = \mathbf{k}_\parallel \times \hat{\mathbf{z}}/|k_\parallel|$ is the unit magnetic polarization vector[7] parallel to the interface (for clarity directions parallel to the interface are here labeled by the two-dimensional (2D) vector $\mathbf{A}_\parallel = [A_x, A_y]$). Applying Maxwell's equations in both media, we also deduce the electric fields $\mathbf{E}_j(\mathbf{r}_\parallel, z) = -(c\mathbf{k}_j/\varepsilon_j\omega) \times \mathbf{H}_j(\mathbf{r}_\parallel, z)$ which have components parallel and perpendicular to the interface. Finally, from Maxwell's equations and the boundary conditions at the interface, we obtain the dispersion relation which is given by[1,2,7]

$$\mathbf{k}_{\parallel}^2 = (\mathbf{k}_{\parallel}' + i\mathbf{k}_{\parallel}'')^2 = k_0^2 \frac{\varepsilon_m \varepsilon_d}{\varepsilon_d + \varepsilon_m}. \tag{C1}$$

From Eq. (C1) we deduce immediately the generalization of Eq. (4),

$$\mathbf{k}_{\parallel}' \cdot \mathbf{k}_{\parallel}'' = \frac{1}{2} \frac{k_0^2 \varepsilon_m'' \varepsilon_d^2}{|\varepsilon_d + \varepsilon_m|^2} > 0. \tag{C2}$$

The inequality holds wherever $\varepsilon_m'' > 0$ is verified and generally means that the angle between $\mathbf{k}_{\parallel}'$ and $\mathbf{k}_{\parallel}''$ is always smaller than 90°.

The calculation of the Poynting vector in the general case of an inhomogeneous SP plane wave has to be treated very carefully since usually the orthogonality condition $\mathbf{k}_{\parallel} \cdot \hat{\mathbf{b}}_{\parallel,j} = 0$ imposed by Maxwell's equations does not imply $\mathbf{k}_{\parallel} \cdot \hat{\mathbf{b}}_{\parallel,j}^* = 0$. This means that

$$\langle \mathbf{S}_j \rangle = \frac{c^2}{2\omega} \mathrm{Re}\left[\frac{\mathbf{q_j}}{\varepsilon_j} - \frac{(\mathbf{k}_{\parallel} \cdot \hat{\mathbf{b}}_{\parallel,j}^*) \hat{\mathbf{b}}_{\parallel,j}}{\varepsilon_j} \right] e^{-2\mathbf{q}'' \cdot \mathbf{r}} \tag{C3}$$

does not reduce to $\langle \mathbf{S}_j \rangle = \frac{c^2}{2\omega} \mathrm{Re}[\frac{\mathbf{q}_j}{\varepsilon_j}] e^{-2\mathbf{q}'' \cdot \mathbf{r}}$ as it is for the homogeneous plane wave (actually, the additional term $\frac{c^2}{\omega |\mathbf{k}_{\parallel}|^2} [(\mathbf{k}_{\parallel}'' \times \mathbf{k}_{\parallel}') \cdot \hat{\boldsymbol{z}}] \mathrm{Im}[\frac{\mathbf{k}_{\parallel}}{\varepsilon_j}] \times \hat{\boldsymbol{z}}$, which contributes to Eq. (C3) only in directions parallel to the interface, vanishes if $\mathbf{k}_{\parallel}'$ and $\mathbf{k}_{\parallel}''$ are collinear, i.e., if the wave is homogeneous). Instead of calculating the explicit form of the Poynting vector, we use here another useful property. Indeed, from the time averaged Poynting theorem in a dissipative medium,[18,20] $\nabla \cdot \langle \mathbf{S} \rangle = -\omega(\varepsilon'' |\mathbf{E}|^2)/2$, we deduce that for any inhomogeneous plane wave with electric field $\mathbf{E} = \mathbf{E}_0 e^{i\mathbf{q} \cdot \mathbf{r}}$ and magnetic field $\mathbf{B} = \frac{\mathbf{q}}{k_0} \times \mathbf{E}_0 e^{i\mathbf{q} \cdot \mathbf{r}}$ we have[47]

$$\mathbf{q}'' \cdot \langle \mathbf{S} \rangle = \omega \varepsilon'' |\mathbf{E}_0|^2 / 4 > 0. \tag{C4}$$

Application of Eq. (C4) to the inhomogeneous SP wave leads to $\mathbf{q}_d'' \cdot \langle \mathbf{S}_d \rangle = 0$ in the dielectric and to $\mathbf{q}_m'' \cdot \langle \mathbf{S}_m \rangle = \omega \varepsilon'' / (4|\varepsilon_m|)$ in the metal. These relations allow us to calculate $\mathbf{k}_{\parallel}'' \cdot \langle \mathbf{S}_{\parallel,j} \rangle$ by knowing $k_{z,j}'' \cdot \langle S_{z,j} \rangle = k_{z,j}'' \frac{c^2}{2\omega} \mathrm{Re}[\frac{k_{z,j}}{\varepsilon_j}] e^{-2\mathbf{q}'' \cdot \mathbf{r}}$. Since $k_{z,j}$ does not depend on $\mathbf{k}_{\parallel}$ (Ref. 22) the scalar product $\mathbf{k}_{\parallel}'' \cdot \langle \mathbf{S}_{\parallel,j} \rangle$ is, up to the positive coefficient $e^{-2\mathbf{q}'' \cdot \mathbf{r}}$, independent of the direction taken by $\mathbf{k}_{\parallel}'$ and $\mathbf{k}_{\parallel}''$ so that the main result of Appendix A remains unchanged and we have finally after integration along z

$$\mathbf{k}_{\parallel}'' \cdot \langle \mathbf{S}_{\parallel}^{\mathrm{total}} \rangle \propto (\tilde{k}_{z,d}'' \tilde{k}_{\mathrm{SP}}'')^2 + (\tilde{k}_{\mathrm{SP}}'' \tilde{k}_{\mathrm{SP}}'')^2 \tilde{\varepsilon}'' > 0, \tag{C5}$$

where $\tilde{k}_{z,d}$ and $\tilde{k}_{\mathrm{SP}}$ have the meanings explained in Appendix A.

[1] H. Raether, *Surface Plasmons* (Springer, Berlin, 1988).
[2] J. Zenneck, Ann. Phys. **23**, 846 (1907).
[3] C. Genet and T. Ebbesen, Nature (London) **445**, 39 (2007).
[4] A. Drezet, A. Hohenau, D. Koller, A. Stepanov, H. Ditlbacher, B. Steinberger, F. Aussenegg, A. Leitner, and J. Krenn, Mater. Sci. Eng., B **149**, 220 (2008).
[5] H. Lamb, Proc. London Math. Soc. **s2-1**, 473 (1904).
[6] V. Veselago, Sov. Phys. Usp. **10**, 509 (1968).
[7] A. V. Kats, S. Savel'ev, V. A. Yampol'skii, and F. Nori, Phys. Rev. Lett. **98**, 073901 (2007).
[8] R. Ruppin, Phys. Lett. A **277**, 61 (2000).
[9] C. Caloz, C.-J. Lee, D. R. Smith, J. B. Pendry, and T. Itoh, Proceedings of the Antennas and Propagation Society International Symposium (IEEE, New York, 2004),Vol. 3, p. 3151.
[10] J. B. Pendry, Phys. Rev. Lett. **85**, 3966 (2000).
[11] F. N. Fang, H. Lee, C. Sun, and X. Zhang, Science **308**, 534 (2005).
[12] V. Shalaev, Nat. Phys. **1**, 41 (2007).
[13] V. A. Podolskiy and E. E. Narimanov, Opt. Lett. **30**, 75 (2005).
[14] H. Shin and S. Fan, Phys. Rev. Lett. **96**, 073907 (2006).
[15] A. Alu and N. Engheta, J. Opt. Soc. Am. B **23**, 571 (2006).
[16] H. Lezec, J. A. Dionne, and H. A. Atwater, Science **316**, 430 (2007).
[17] I. I. Smolyaninov, Y.-J. Hung, and C. C. Davis, Science **315**, 1699 (2007).
[18] L. D. Landau, E. M. Lifschitz, and L. P. Pitaevskii, *Electrodynamics of Continuous Media*, 2nd ed. (Pergamon, New York, 1984).
[19] M. I. Stockman, Phys. Rev. Lett. **98**, 177404 (2007).
[20] J. D. Jackson, *Classical Electrodynamics*, 3rd ed. (Wiley, New York, 1999).
[21] L. Brillouin, *Wave Propagation and Group Velocity* (Academic, New York, 1960).
[22] We note (Ref. 1) that the component of the SP wave vector along the normal to the interface is given by the formula $k_{z,j} = k_{z,j}' + ik_{z,j}'' = \pm k_0 \sqrt{\frac{\varepsilon_j^2}{\varepsilon_d + \varepsilon_m}}$. The choice of the sign $\pm$ in this equation is done in order to confine the SP wave along the interface, i.e., $k_{z,d}'' > 0$ and $k_{z,m}'' < 0$.
[23] The integrated energy fluxes in the metal and the dielectric are $\int_{-\infty}^{0} \langle S_x^m \rangle dz = -\frac{c e^{-2k_{\mathrm{SP}}'' x}}{2k_0} \frac{k_{\mathrm{SP}}' \varepsilon_m' + k_{\mathrm{SP}}'' \varepsilon_m''}{2k_{z,m}'' |\varepsilon_m|^2}$ and $\int_{0}^{+\infty} \langle S_x^d \rangle dz = \frac{c e^{-2k_{\mathrm{SP}}'' x}}{2k_0} \frac{k_{\mathrm{SP}}'}{2k_{z,d}'' \varepsilon_d}$.
[24] To calculate exact values for $l(t)$ is problematic when using the experimental values of Ref. 48 for the metal dielectric function, as they have to be interpolated. This usually leads to oscillations and/or discontinuities in the second derivative of $d^2\omega / dk_{\mathrm{SP}}^2$.
[25] A. Sommerfeld, Phys. Z. **8**, 841 (1907).
[26] C. Garrett and D. McCumber, Phys. Rev. A **1**, 305 (1970).
[27] S. Chu and S. Wong, Phys. Rev. Lett. **48**, 738 (1982).
[28] J. Stratton, *Electromagnetic Theory* (McGraw-Hill, New York, 1941).
[29] G. Dolling, C. Enkrich, M. Wegener, C. Soukoulis, and S. Linden, Rev. Sci. Instrum. **312**, 892 (2006).
[30] G. M. Gehring, A. Schweinsberg, C. Barsi, N. Kostinski, and R. W. Boyd, Science **312**, 895 (2006).
[31] D. J. Gauthier and R. W. Boyd, Photonics Spectra **41**, 82 (2007).
[32] S. Stallinga, Phys. Rev. E **73**, 026606 (2006).
[33] J. Elser and V. A. Podolskiy, Phys. Rev. Lett. **100**, 066402 (2008).
[34] R. F. Oulton, D. F. P. Pile, Y. Liu, and X. Zhang, Phys. Rev. B **76**, 035408 (2007).

[35] In the present paper the angle α between the averaged Poynting vector and $\mathbf{k}''$ and the angle β between $\mathbf{k}'$ and $\mathbf{k}''$ in the refraction side are very close to 45° but slightly different: $\alpha=44.04°$ and $\beta=44.66°$.

[36] Rigorously speaking this SP wave corresponds to a Lorentz distribution in Eq. (8). However, since the SP propagation length $L_{SP}=21$ μm on the silver /air interface is much larger than the SP wavelength, we can neglect this effect to simplify the calculation. Here we consider the wave vector real for $x<0$, i.e., $k_{SP,Ag}=k'_{SP,Ag}=k_0\,\mathrm{Re}[\sqrt{\frac{\varepsilon_{Au}}{1+\varepsilon_{Au}}}]$.

[37] P. Tournois and V. Laude, Opt. Commun. **137**, 41 (1997).

[38] E. N. Economou, Phys. Rev. **182**, 539 (1969).

[39] J. J. Burke, G. I. Stegeman, and T. Tamir, Phys. Rev. B **33**, 5186 (1986).

[40] R. Depine and A. Lakhtakia, Microwave Opt. Technol. Lett. **41**, 315 (2004).

[41] S. Ramakrishna and O. Martin, Opt. Lett. **30**, 2626 (2005).

[42] R. W. Ziolkowski and E. Heyman, Phys. Rev. E **64**, 056625 (2001).

[43] J. Skaar, Opt. Lett. **31**, 3372 (2006).

[44] A. A. Govyadinov, V. A. Podolskiy, and M. A. Noginov, Appl. Phys. Lett. **91**, 191103 (2007).

[45] P. Kinsler and M. McCall, Microwave Opt. Technol. Lett. **50**, 1804 (2008).

[46] P. M. Morse and H. Feshbach, *Methods of Theoretical Physics* (McGraw-Hill, New York, 1953), Pts. 1 and 2.

[47] The proof goes as follows. Consider a circular cylinder of length L with symmetry axis along the direction defined by $\mathbf{q}''$. Let us call A and B the terminal disks closing the surface defined by this cylinder ($\mathbf{q}''$ goes in the direction $\overrightarrow{AB}$). Then application of Poynting theorem in this cylindrical volume together with the use of Gauss theorem leads to the relation $-\int_A \hat{\mathbf{q}}''\cdot\langle\mathbf{S}\rangle d\sigma + \int_B \hat{\mathbf{q}}''\cdot\langle\mathbf{S}\rangle d\sigma + \int_{\text{lateral}}\mathbf{d}\sigma\cdot\langle\mathbf{S}\rangle = -\int_V \omega(\varepsilon''|\mathbf{E}|^2)/2dV$, where $\hat{\mathbf{q}}''$ is the unit vector $\mathbf{q}''/|\mathbf{q}''|$. This integral simplifies since on the lateral surface the flux vanishes (the surface terms located on opposite points of a given section of the cylinder annihilate each other two per two). Taking then the limits $L=\infty$ (i.e., rejecting B at infinity) gives after volume integration formula (C4).

[48] P. Johnson and R. Christy, Phys. Rev. B **6**, 4370 (1972).